Journal of Experimental Botany, Vol. 60, No. 6, pp. 1743–1757, 2009
doi:10.1093/jxb/erp044 Advance Access publication 5 March, 2009
This paper is available online free of all access charges (see http://jxb.oxfordjournals.org/open_access.html for further details)

Journal of Experimental Botany
www.jxb.oxfordjournals.org

RESEARCH PAPER

Biochemical characterization, mitochondrial localization, expression, and potential functions for an *Arabidopsis* γ-aminobutyrate transaminase that utilizes both pyruvate and glyoxylate

Shawn M. Clark[1], Rosa Di Leo[1], Preetinder K. Dhanoa[2], Owen R. Van Cauwenberghe[1,*], Robert T. Mullen[2] and Barry J. Shelp[1,§]

[1] Department of Plant Agriculture, University of Guelph, Guelph, Ontario, Canada N1G 2W1
[2] Department of Molecular and Cellular Biology, University of Guelph, Guelph, Ontario, Canada N1G 2W1

Received 25 November 2008; Revised 31 January 2009; Accepted 4 February 2009

Abstract

γ-Aminobutyrate transaminase (GABA-T) catalyses the breakdown of GABA to succinic semialdehyde. In this report, the previously identified *Arabidopsis thaliana* (L.) Heyhn GABA-T (*At*GABA-T) was characterized in more detail. Full-length *At*GABA-T contains an N-terminal 36 amino acid long targeting pre-sequence (36 amino acids) that is both sufficient and necessary for targeting the enzyme to mitochondria. Removal of the pre-sequence encoding this N-terminal targeting domain and co-expression of the resulting truncated *AtGABA-T* cDNA with the GroES/EL molecular chaperone complex in *Escherichia coli* yielded good recovery of the soluble recombinant proteins. Activity assays indicated that purified recombinant GABA-T has both pyruvate- and glyoxylate-dependent activities, but cannot utilize 2-oxoglutarate as amino acceptor. Kinetic parameters for glyoxylate- and pyruvate-dependent GABA-T activities were similar, with physiologically relevant affinities. Assays of GABA-T activity in cell-free leaf extracts from wild-type *Arabidopsis* and two knockout mutants in different genetic backgrounds confirmed that the native enzyme possesses both pyruvate- and glyoxylate-dependent activities. The GABA-T transcript was present throughout the plant, but its expression was highest in roots and increased as a function of leaf development. A GABA-T with dual functions suggests the potential for interaction between GABA metabolism and photorespiratory glyoxylate production.

Key words: Enzyme kinetics, GABA transaminase, gene expression, Glyoxylate, Photorespiration, Recombinant protein, Subcellular localization.

Introduction

γ-Aminobutyric acid (GABA) is a ubiquitous four C, non-protein amino acid found in prokaryotes and eukaryotes (Satya Narayan and Nair, 1990; Shelp *et al.*, 1999). It was first identified in potato tubers during the 1950s, and has since been characterized as a neural inhibitor in the central nervous system of mammals. A model for the function of GABA in plants remains elusive, despite evidence linking the metabolite to both stress and signalling (Shelp *et al.*, 1999, 2006; Bouché and Fromm, 2004; Fait *et al.*, 2008).

GABA is produced in the cytosol (Breitkreuz and Shelp, 1995) via the decarboxylation of glutamate in a reaction catalysed by glutamate decarboxylase, a calcium/

* Present address: Lilly Analytical Research Laboratory, Eli Lilly Canada Inc., 3650 Danforth Avenue, Toronto, ON M1N 2E8, Canada
§ To whom correspondence should be addressed. E-mail: bshelp@uoguelph.ca

Abbreviations: BY-2, Bright Yellow-2; CAT, chloramphenicol acyltransferase; GABA, γ-aminobutyric acid; GABA-T, γ-aminobutyrate transaminase; GFP, green fluorescent protein; ORF, open reading frame; PCR, polymerase chain reaction; SDS-PAGE, sodium dodecyl sulphate-polyacrylamide gel electrophoresis; SSA, succinic semialdehyde; SSADH, succinic semialdehyde dehydrogenase.

calmodulin-dependent enzyme (Baum *et al.*, 1993; Ling *et al.*, 1994; Snedden *et al.*, 1995, 1996). GABA is then transaminated to succinic semialdehyde (SSA) via GABA-transaminase (GABA-T) in the mitochondrion (Van Cauwenberghe and Shelp, 1999; Van Cauwenberghe *et al.*, 2002). SSA is oxidized to succinate via SSA dehydrogenase (SSADH) in the mitochondrion (Breitkreuz and Shelp, 1995; Busch and Fromm, 1999), or reduced to γ-hydroxybutyrate by SSA reductase activities in the cytosol and chloroplast (Allan *et al.*, 2003, 2008; Breitkreuz *et al.*, 2003; Fait *et al.*, 2005; Allan and Shelp, 2006; Hoover *et al.*, 2007; Simpson *et al.*, 2008).

GABA-T activity in plants differs from that in most other organisms. GABA-T in mammals, yeast, and *Escherichia coli* uses 2-oxoglutarate exclusively as an amino donor (André and Jauniaux, 1990; Bartsch *et al.*, 1990; De Biase *et al.*, 1995), whereas both pyruvate- and 2-oxoglutarate-dependent activities occur in plants (Shelp *et al.*, 1995; Van Cauwenberghe and Shelp, 1999). The 2-oxoglutarate-dependent activity from tobacco is highly unstable during purification, and production of a purified protein has not been possible (Van Cauwenberghe and Shelp, 1999). However, the pyruvate-dependent activity has been purified to homogeneity, thereby enabling partial amino acid sequencing and identification of an *Arabidopsis* (designated hereinafter as *At*GABA-T) cDNA (Van Cauwenberghe *et al.*, 2002). Recombinant expression of the cDNA in *E. coli* confirmed that it encodes a pyruvate-dependent GABA-T that lacks detectable 2-oxoglutarate-dependent activity. Recombinant expression of the protein was minimal and primarily insoluble, making more detailed analysis of the enzyme impracticable (Van Cauwenberghe *et al.*, 2002). Prediction of subcellular localization using PSORT (Nakai and Kanehisa, 1992) suggested that *At*GABA-T, like the mammalian enzyme, contains an N-terminal mitochondrial matrix targeting signal (Van Cauwenberghe *et al.*, 2002), which is in agreement with a previous subcellular fractionation study of soybean protoplasts (Breitkreuz and Shelp, 1995).

In this study, a truncated *At*GABA-T cDNA lacking the putative N-terminal targeting pre-sequence was co-expressed with the molecular chaperones GroES/EL in *E. coli.* Substrate specificity and kinetic studies revealed that the recombinant enzyme utilizes only GABA as the amino donor in the production of SSA. As previously observed, the enzyme used pyruvate but not 2-oxoglutarate as an amino acceptor (Van Cauwenberghe *et al.*, 2002). In addition, the enzyme was found to have previously unreported glyoxylate-dependent GABA-T activity. A transient expression system, confirmed that *At*GABA-T is localized to mitochondria, and that proper sorting of the enzyme does require an N-terminal targeting pre-sequence. The use of knockout mutants of *Arabidopsis* confirmed that the native enzyme utilizes both pyruvate and glyoxylate as amino acceptors and suggested that there is no 2-oxoglutarate-dependent GABA-T activity in *Arabidopsis*.

Materials and methods

Production, purification, and analysis of recombinant Arabidopsis *GABA-T*

The full-length cDNA of an *Arabidopsis thaliana* (L.) Heynh GABA-T (GenBank accession no. AF351125), with or without its mitochondrial targeting domain (predicted to be 36 N-terminal amino acids based on the location of the mitochondrial cleavage site) was cloned into the pET-15b expression vector (includes a His_6 tag on the N-terminus; Novagen, San Diego, CA, USA) using standard techniques (Sambrook *et al.*, 1989). The no-target GABA-T was amplified for plasmid ligation using primers 5′ GGA ATT CCA TAT GAC TAC TGA GGC AGC ACC TG 3′ and 5′ GCG GGA TCC TCA CTT CTT GTG CTG AGC C 3′.

Full-length and truncated GABA-T was expressed in *E. coli* BL-21(DE3) Rosetta (pLysS) cells (Novagen) carrying the pREP4-GroESL vector (Dale *et al.*, 1994). Cells were grown at 37 °C and 225 rpm in Luria–Bertani broth containing 50 μg ml^{-1} ampicillin, 34 μg ml^{-1} chloramphenicol, and 30 μg ml^{-1} kanamycin, to an OD_{600} of 0.6. Cultures were cooled to 25 °C, isopropyl-β-D-thiogalatopyranoside (IPTG) was added to a concentration of 0.25 mM, and the cultures were shaken at 225 rpm and 25 °C for 2 h. Cells were pelleted by centrifugation at 3000 *g* at 4 °C for 10 min and stored at –80 °C for 1–2 weeks.

Pellets containing recombinant protein were suspended in 10 ml of 50 mM TRIS-HCl (pH 8.2), 1 mM EDTA, 0.5 M NaCl, 0.5 mM phenylmethylsulphonyl fluoride (PMSF), 1 μg ml^{-1} pepstatin A, 2 μg ml^{-1} leupeptin, 10 mM imidazole, and 10% glycerol. Lysozyme was added to 1 mg ml^{-1} and the mixture was incubated on ice with gentle shaking. After 30 min, 6 mM 3-[3-cholamidopropyl)dimethylammonio]-1-propanesulphonate (CHAPS) was added and the mixture was shaken for a further 30 min. Then the mixture was made up to 10 mM $MgCl_2$ and 5 mM ATP, a few DNase crystals added, and incubated at room temperature for 20 min with gentle rocking, followed by centrifugation at 3000 *g* and 4 °C for 10 min. The supernatant was collected and passed over ProBond nickel resin (Invitrogen, Carlsbad, CA, USA) equilibrated with 50 mM TRIS-HCl (pH 8.2) and 0.5 M NaCl. The nickel resin was washed with 50 mM TRIS-HCl (pH 8.2) containing 20 mM imidazole and 10% glycerol, and the recombinant protein was eluted with 50 mM TRIS-HCl (pH 8.2) containing 500 mM imidazole and 10% glycerol. Pyridoxal-5-phosphate at 2 μg ml^{-1} was added to all buffers used in the purification of the full or truncated GABA-T. Protein concentration in the eluate was determined using the Bradford assay method (Bradford, 1976). For visual confirmation, 12% sodium dodecyl sulphate-polyacrylamide gel electrophoresis (SDS-PAGE) was carried out with 10 μl protein samples and standard protocols, and then the gels were stained with Coomassie brilliant blue R250 (Sambrook *et al.*, 1989; Van Cauwenberghe *et al.*, 2002). Immunoblotting was carried out according to standard protocols (Sambrook *et al.*, 1989) using the HisTag monoclonal antibody (Novagen), the

anti-mouse antibody (Sigma-Aldrich, Oakville, ON, Canada), and the alkaline phosphatase conjugate substrate kit (BioRad Laboratories, Hercules, CA, USA) for detection. Molecular weight standards were purchased from Fermentas (Burlington, ON, Canada).

The standard activity assay contained 50 mM *N*-tris(hydroxymethyl)methyl-4-aminobutanesulphonic acid (TABS; pH 9), 1.5 mM dithiothreitol (DTT), 0.625 mM EDTA, 0.1 mM pyridoxal-5-phosphate, 10% glycerol, and 0.5 µl of purified recombinant protein or 50 µl of desalted crude leaf extract, and was conducted at 30 °C. A discontinuous assay used a final volume of 500 µl and 1 mM amino acceptor; the reaction was initiated by the addition of 1 mM amino donor or water (control), incubated in a water bath for 15 min and 3 h, for determination of the specific activity and substrate specificity or leaf activity, respectively, and then terminated by the addition of ice-cold sulphosalicylic acid to 60 mM (Van Cauwenberghe and Shelp, 1999). The supernatant was neutralized with 1 N NaOH, and the production of specific amino acids was monitored via reverse-phase HPLC as described previously (Allan and Shelp, 2006). A continuous assay used a final volume of 800 µl and contained 125 µM NAD or NADH; the reaction was initiated by the addition of an appropriate amino donor. The influence of pH on enzyme activity was determined at 2 mM pyruvate and 8 mM GABA using 50 mM *N*-tris[hydroxymethyl]-methyl-2-aminoethane-sulphonic acid (pH 7.5–8.2), 50 mM TABS (pH 8.2–9.5), and 50 mM 3-(cyclohexylamino)-1-propanesulphonic acid (pH 9.5–10.5). Substrates were tested at pH 9 over the following concentration range to determine K_m and V_{max} values: pyruvate, 0.00625–2 mM; GABA, 0.0125–8 mM; glyoxylate, 0.00625–2 mM; alanine, 0.05–16 mM; and SSA, 0.005–0.5 mM. The following inhibitors of the forward reaction were tested with 2 mM pyruvate and 0.5–4 mM GABA: β-alanine, 0.5–2 mM; ornithine, 0.25–1 mM; glycine, 0.5–4 mM; and vigabatrin, 0.5–2 mM. Reactions that generate SSA and pyruvate were coupled to NAD-dependent SSADH (1.14 U or 50 µg ml^{-1} SSADH) (see Supplementary Materials and methods and Supplementary Fig. S1 available at *JXB* online) and NADH-dependent lactate dehydrogenase (LDH; 1 U or 31.25 µg ml^{-1}, hog muscle, Boehringer Mannheim, Burlington, Canada), respectively. The rate of each reaction was monitored as the change in NADH concentration at 340 nm using a Beckman DU640 Spectrophotometer (Mississauga, Canada) equipped with temperature control. All assays were conducted in triplicate. Kinetic parameters were calculated using non-linear least-squares analysis (SigmaPlot2000, version 6.1; Enzyme Kinetics Module, version 1.0; Systat Software Inc., Point Richmond, CA, USA). Inhibition data were fit to appropriate forms of the Michaelis–Menten equation using non-linear least-squares analysis. The inhibition constant, K_i, and the mode of inhibition for each product were confirmed by secondary plots of slopes and intercepts from the double-reciprocal transformation. The equilibrium coefficient was calculated according to Van Bemmelen *et al.* (1985) using the following equation:

$$k_{Eq} = {k_{catf}}^2 / {k_{catr}}^2 \times \left(K_{m(SSA)} \times K_{m(Ala)}\right) / \left(K_{m(GABA)} \times K_{m(pyruvate)}\right)$$

where f and r represent the forward and reverse reactions, respectively.

Expression and activity of native Arabidopsis *GABA-T*

The *Arabidopsis* knockout lines used in this study, POP2-3 (CS6387) and GABAT1-1 (Salk_007661) (ecotypes Columbia and Wassilewskija, respectively), have been characterized by Palanivelu *et al.* (2003) and Miyashita and Good (2008), respectively. All wild-type and knockout *Arabidopsis* plants were grown in controlled-environment chambers (Ecological Chambers Inc., Model GC8-2H, Winnipeg, Canada) set at 23/19 °C day/night temperatures, a photosynthetic photon flux density of 150 µmol m^{-2} s^{-1} at the top of the seedling trays (supplied by cool white fluorescent lighting, Sylvania, Mississauga, Canada), and 65% relative humidity, and supplied as necessary with tap water. For analysis of gene expression, *Arabidopsis* Columbia plants were grown in a Fox sandy loam (pH 6.5) under a 14 h photoperiod (i.e. long day conditions) and supplied once weekly with a modified quarter-strength nutrient solution (Shelp *et al.*, 1992), and total RNA was isolated using the Qiagen RNeasy kit (Qiagen, Mississauga, Canada). The bottom four leaves of the rosette were harvested for RNA extraction at 2 (young), 4.5 (mature), and 10 (senescent) weeks, whereas root, stem, and flower samples were collected at 6 weeks. For analysis of amino acid composition and *in vitro* analysis of enzyme activity in mature leaves, plants were grown for 4 weeks in Sunshine professional growth mix (Sun Gro Horticulture Canada, Seba Beach, Alberta) under a 10 h photoperiod (i.e. short day conditions), and not supplied with fertilizer. Amino acid profiles were determined via reverse-phase HPLC as described previously (Allan and Shelp, 2006).

Real-time polymerase chain reaction (PCR) was preformed using the Platinum SYBR Green qPCR SuperMix UDG (Invitrogen) with a BioRad iCycler (Hercules, CA, USA). The following pairs of gene-specific primers were used to amplify the GABA-T gene (5′ TGG ATC AGA TGC CAA CGA TA 3′ and 5′ GTG GAG CCA TGG TAC GAT TT 3′) and the 18S rRNA gene (5′ TCT GGC TTG CTC TGA TGA TT 3′ and 5′ TCG AAA GTT GAT AGG GCA GA 3′). Total RNA was treated with Turbo DNase (Ambion, Austin, TX, USA). For cDNA synthesis, 300 ng of total RNA were incubated with 1 µl of random hexamer primers, brought up to 15 µl with RNase free water, incubated at 75 °C for 10 min, and chilled on ice. A 2 µl aliquot of 10× reaction buffer, 40 U of RNase inhibitor (Ambion), and 10 nM dNTPs were added and then incubated at 25 °C for 10 min. One hundred units of M-MLV reverse (Ambion) were added to bring the final reaction volume to 20 µl, then the reaction was incubated at 37 °C for 1 h and inactivated at 95 °C for 10 min. Each quantitative PCR used 1× SYBR Green qPCR mix, 0.2 µM forward and reverse primers, and 1 µl of cDNA in a 20 µl volume. All tubes were subjected to 3 min at 95 °C, followed by 40 cycles of 95 °C for 20 s, 60 °C for 20 s, and

72 °C for 20 s. SYBR Green absorbance was detected at 72 °C, and all reactions were conducted in triplicate. GABA-T expression in each sample was normalized to the level of 18S rRNA (Nicot *et al.*, 2005).

Cell-free extracts were prepared by grinding leaf material in 5 vols of ice-cold 50 mM TRIS-HCl buffer (pH 8.2) containing 3 mM DTT, 1.25 mM EDTA, 2.5 mM $MgCl_2$, 10% glycerol, 6 mM CHAPS, 2 μg ml^{-1} pyridoxal-5-phosphate, 1 mM PMSF, and 2.5 μg ml^{-1} leupeptin and pepstatin A. The homogenate was incubated on ice for 20 min with gentle rocking and then centrifuged at 3000 *g* for 10 min at 4 °C, and the supernatant was desalted using a Zebra desalt spin column (Pierce, Rockford, IL, USA). The total protein concentration was determined using the Bradford assay method (Bradford, 1976). GABA-T activity was measured as described above.

Wild-type and knockout GABA-T plants were grown on three types of half-strength MS medium: (i) standard MS medium containing N; (ii) MS medium with 10 mM GABA as the sole N source; and (iii) MS medium containing no N and 10 mM potassium sulphate.

Transient expression and subcellular localization of Arabidopsis *GABA-T in tobacco BY-2 cells*

Four plant expression plasmids containing *At*GABA-T, or a modified version thereof, were constructed for this study including: (i) pUC18/*At*GABA-T–GFP, encoding the entire open reading frame (ORF) of *At*GABA-T fused to the N-terminus of the green fluorescent protein (GFP); (ii) pRTL2/*At*GABA-T-myc, encoding the entire ORF of *At*GABA-T fused at its C-terminus to the myc epitope tag (Fritze and Anderson, 2000); (iii) pUC18/1–46-*At*GABA-T–GFP, encoding the N-terminal 46 amino acids of *At*GABA-T, which represents the protein's predicted mitochondrial matrix targeting pre-sequence fused to the N-terminus of GFP; and (iv) pUC18/1–46Δ*At*GABA-T–GFP, encoding an N-terminal truncated version of the fusion protein *At*GABA-T–GFP lacking the N-terminal amino acids 1–46 of *At*GABA-T. Construction of these four plasmids was carried out by amplifying (via PCR) each of the above-mentioned *At*GABA-T sequences with appropriate forward and reverse primers that introduced a 5′ and 3′ *Nhe*I site (for primer sequences refer to Supplementary Table S1 at *JXB* online). The PCR products were subcloned into pCR2.1 (Invitrogen), and the resulting plasmids were digested with *Nhe*I. The *Nhe*I DNA fragments were then ligated into either *Nhe*I-digested pUC18/NheI–GFP, yielding pUC18/AtGABA-T–GFP or pUC18/1–46-*At*GABA-T–GFP, or *Nhe*I-digested pRTL2/*Nhe*I-myc, yielding pRLT2/*At*GABA-T-myc or pRLT2/1–46*At*ΔGABA-T-myc.

The plasmid pUC18/*Nhe*I-GFP is a general purpose GFP fusion cassette whereby an in-frame *Nhe*I site was introduced at the 5′ end of the GFP ORF using PCR site-directed mutagenesis along with the appropriate (complementary) mutagenic forward (5′ GAC GAC CTG CAG GTC GAC GCT AGC ATG GTG AGC AAG GGC 3′) and reverse (5′ GCC CTT GCT CAC CAG CTA GCC GTC GAC CTG CAG GTC GTC 3′) primers and pUC18/GFP as template DNA (Chiu *et al.*, 1996). pRTL2/*Nhe*I-myc, a modified version of the plant expression vector pRTL2/myc-*Xba*I (Murphy *et al.*, 2003), was constructed in two steps. First, sequences encoding the *Xba*I site downstream of the myc epitope tag (-EQKLISEEDL-; Fritze and Anderson, 2000) were modified (via PCR mutagenesis) to encode a stop codon. Sequences of the (complementary) mutagenic primers used in this PCR were (forward) 5′ GAA GAT CTG TCT TGA ACT CCG CAA AAA TCA CC 3′) and (reverse) 5′ GGT GAT TTT TGC GGA CTT CAA GAC AGA TCT TC 3′. Secondly, the resulting plasmid pRTL2/myc-stop was modified (via PCR mutagenesis) using the complementary forward (5′ CTA GAA CGC TAG CAT GGA ACA AAA GTT G 3′) and reverse (5′ CAA CTT TTG TTC CAT GCT AGC GTT CTA G 3′) primers to introduce a unique in-frame *Nhe*I site immediately upstream of the myc epitope sequence, yielding pRLT2/*Nhe*I-myc. pBIN35SB60catE9, encoding the N-terminal pre-sequence of the β-subunit of F_1-ATPase from *Nicotiana plumaginfolia* L. fused to the N-terminus of the bacterial passenger protein chloramphenicol acyltransferase (CAT) and serving as a well-established mitochondrial marker protein, was provided by F Chaumont (University of Lauvain, Place Croix de Sud, Belgium) (Chaumont *et al.*, 1994).

Tobacco (*Nicotiana tabacum* L.) Bright Yellow-2 (BY-2) cells were maintained and prepared for biolistic bombardment as described previously by Banjoko and Trelease (1995). Transient transformations were performed using the Biolistic Particle Delivery System (Bio-Rad) with either 10 μg or 5 μg of plasmid DNA for individual or co-transformations, respectively. Bombarded cells were incubated at 26 °C for ~20 h in covered Petri dishes to allow transient expression of introduced gene(s) and protein sorting within the cells.

Bombarded BY-2 cells were processed for immunofluorescence microscopy as described by Trelease *et al.* (1996). Briefly, cells were fixed in formaldehyde and permeabilized with pectolyase Y-23 (Kyowa Chemical Products, Osaka, Japan) and Triton X-100. For experiments designed to demonstrate the mitochondrial import of transiently expressed *At*GABA-T-myc, fixed and pecytolyase-treated cells were differentially permeabilized with digitonin (25 μg ml^{-1}) (Sigma Alrich Ltd), rather than Triton X-100, to perforate the plasma membrane, but not organelle membranes (Lee *et al.*, 1997).

Primary and fluorescent dye-conjugated secondary antibodies and sources were as follows: mouse anti-myc (clone 9E10) in hybridoma medium (Princeton University; Monoclonal Antibody Facility, Hybridoma, Princeton, NJ, USA); mouse anti-CAT IgGs (kindly provided by S Subramani, University of California, San Diego, CA, USA); mouse anti-α-tubulin monoclonal antibody (clone DM1A) (Sigma-Aldrich Ltd); rabbit-pea E1β (Luethy *et al.*, 1995); goat anti-mouse Alexa Fluor 488; goat anti-rabbit Alexa Flour 488 (Cedar Lane Laboratories Ltd, Burlington, ON, Canada); and goat anti-rabbit rhodamine red-X (Jackson ImmunoResarch Laboratories Inc., West Grove, PA, USA).

Microscopic visualization of labelled BY-2 cells was performed with a Zeiss Axioskop 2 MOT epifluorescence

microscope (Carl Zeiss Inc., Thornwood, NY, USA) with a Zeiss 63× Plan Apochromat oil immersion objective (Carl Zeiss) and a Retiga 1300 charge-coupled device camera (Qimaging, Burnaby, BC, Canada). All images shown were deconvolved and adjusted for brightness and contrast using Northern Eclipse 5.0 software (Empix Imaging Inc., Mississauga, ON, Canada), and then composed into figures using Adobe Photoshop 8.0 (Adobe Systems, San Jose, CA, USA). The images shown are representative of data obtained from viewing several (>50) transformed BY-2 tobacco cells from at least two separate biolistic bombardment experiments.

Results

Production and characterization of recombinant Arabidopsis *GABA-T*

Initial attempts to express the full-length *At*GABA-T protein in *E. coli* were unsuccessful due to the production of insoluble protein aggregates (data not shown). Co-expression of the GroES/GroEL chaperone complex from the pREP4-GroESL plasmid allowed for recovery of a small proportion of the recombinant protein in the soluble fraction (Fig. 1A). Removal of the protein's putative N-terminal mitochondrial targeting pre-sequence at the site of a predicted R-3 mitochondrial cleavage site (36 amino acids) (Sjöling and Glaser, 1998) dramatically improved the proportion of total protein recovered in the soluble fraction (Fig. 1B). Immunoblot analysis of total crude protein, probed with an α-Histag antibody, revealed a single recombinant truncated *At*GABA-T band at approximately the predicted molecular mass of 53.4 kDa (Fig. 1C, D). Discontinuous assays revealed that the inability of the enzyme to utilize 2-oxogluarate as an amino acceptor was unchanged by removal of the targeting pre-sequence (Table 1). Furthermore, the mean specific activity (±SE of three biological preparations) for the truncated protein (13.4±0.2 μmol mg^{-1} protein min^{-1}) was three times that for the full-length protein (4.5±0.2 μmol mg^{-1} protein min^{-1}), as

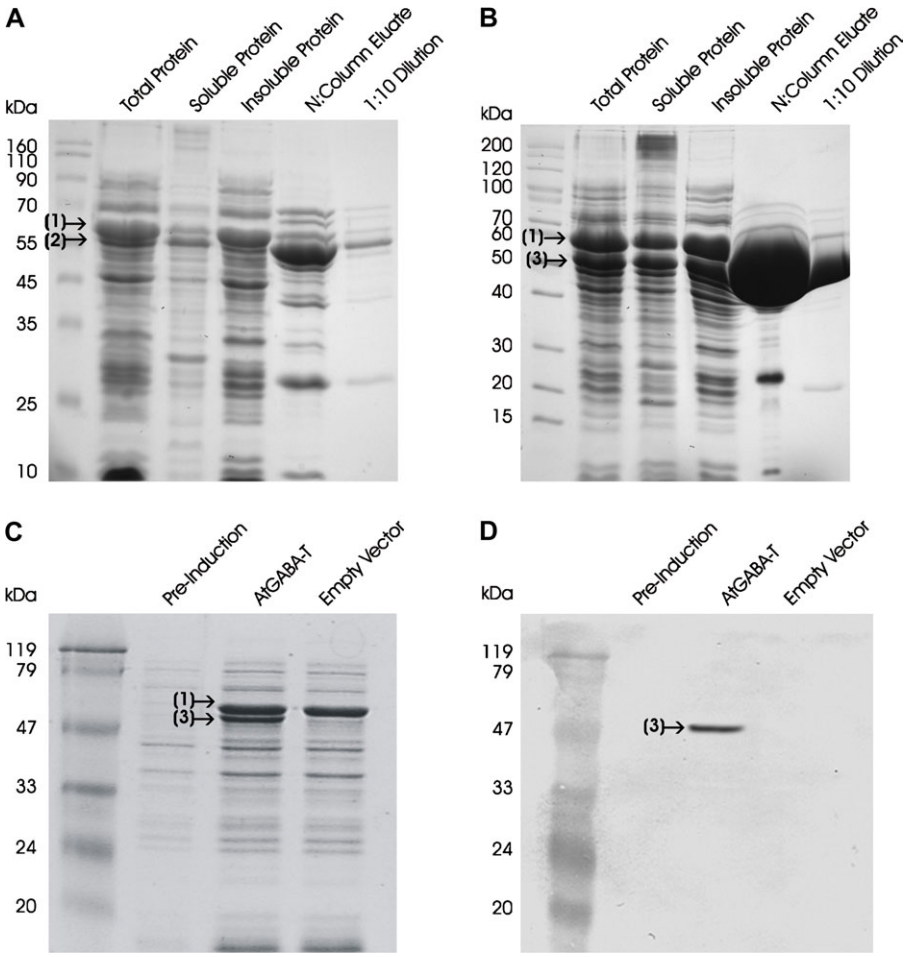

Fig. 1. SDS-PAGE analysis of expression and purification of the full-length recombinant *At*GABA-T (A) or the truncated recombinant *At*GABA-T lacking the mitochondrial targeting domain (B) from *E. coli* BL21 (DE3) Rosetta pLysS cells co-expressing the GroES/EL chaperone complex. (1) The GroEL subunit of the chaperone complex (60 kDa), (2) the full-length *At*GABA-T (57.5 kDa), and (3) the truncated *At*GABA-T (53.4 kDa) are indicated on the gels. The right-hand lane on each gel represents the column eluate diluted 10-fold. SDS-PAGE (C) and immunoblot (D) analyses of total crude protein from BL21 (DE3) Rosetta pLysS cells co-expressing the GroES/EL chaperone complex, and either the empty vector or the truncated recombinant *At*GABA-T. The immunoblot was probed with a HisTag antibody.

Table 1. Pyruvate- and glyoxylate-specific GABA-T activities associated with purified full-length or truncated (lacking the targeting domain) recombinant *Arabidopsis* protein, and crude cell-free *Arabidopsis* leaf extract

Data represent the mean ±SE of triplicate measurements from a typical preparation. Amino acid production was determined via reverse-phase HPLC, and the detection limit for the method was ~0.02 nmol h^{-1}; ND indicates not detectable.

Enzyme source	Amino acceptor	GABA-dependent activity	
		nmol min^{-1} mg^{-1} protein	nmol h^{-1}
Recombinant full-length protein	Pyruvate	3530±90	847±21
	2-Oxoglutarate	ND	ND
Recombinant truncated protein	Pyruvate	7540±360	1810±85
	2-Oxoglutarate	ND	ND
Arabidopsis crude extract	Pyruvate	0.422±0.003	54.7±0.4
	2-Oxoglutarate	0.013±0.003	1.8±0.4

measured by the continuous assay. Thus, the truncated form of the recombinant enzyme was used for the kinetic experiments described herein.

The pH optimum for *At*GABA-T in the forward reaction was ~9.0 (Fig. 2). Preliminary study of the substrate specificity at pH 9 via HPLC analysis of amino acid products revealed that the enzyme utilized glyoxylate, as well as pyruvate, as amino acceptors in the forward reaction, and GABA, but not β-alanine, ornithine, acetylornithine, serine, glycine, asparagine, glutamine, glutamate, valine, leucine, isoleucine, methionine, phenylalanine, histidine, lysine, arginine, aspartate, threonine, tyrosine, tryptophan, proline, or cysteine as amino donors (data not shown). All kinetic parameters for GABA, including specificity constants (i.e. k_{cat}/K_m), were similar in the presence of pyruvate and glyoxylate (Table 2, see also Supplementary Fig. S2 at *JXB* online). The kinetic parameters for pyruvate and glyoxylate were also similar in the presence of GABA. The pyruvate-dependent GABA-T reaction was reversible, whereas the glyoxylate-dependent reaction was not, although glyoxylate could also be used in conjunction with alanine as a substrate in the reverse reaction. The affinity for alanine in the reverse reaction was an order of a magnitude lower than that for GABA in the forward reaction, resulting in specificity constants that were also lower (Table 2; see also Supplementary Fig. S3 at *JXB* online). In contrast, the affinity and specificity constant for SSA were an order of magnitude higher than the same parameters for the other amino acceptors tested in either the reverse or forward directions. The calculated equilibrium ratio for the reversible pyruvate-dependent GABA-T reaction was 0.68. β-Alanine, ornithine, and vigabatrin were effective competitive inhibitors of pyruvate-dependent GABA-T activity, with K_i values similar to the K_m for GABA. Glycine was a slightly less effective inhibitor, with a K_i value in the same range as the K_m for alanine (Table 3; see also Supplementary Fig. S4 at *JXB* online).

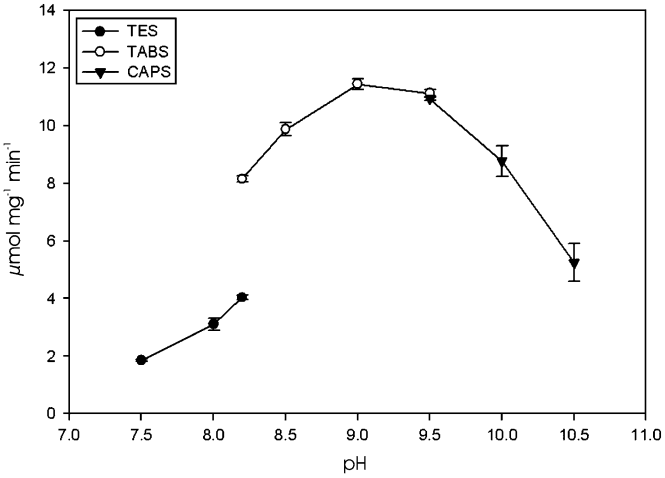

Fig. 2. Dependence of pyruvate-dependent *At*GABA-T activity on pH. Data represent the mean ±SE of triplicate measurements using a typical enzyme preparation; where SE is not shown, it is within the symbol. Three overlapping buffers were used: *N*-tris[hydroxymethyl]-methyl-2-aminoethane-sulphonic acid (filled circles); *N*-tris(hydroxymethyl)methyl-4-aminobutanesulphonic acid (open circles); and, 3-(cyclohexylamino)-1-propanesulphonic acid (inverted triangles).

Table 2. Kinetic parameters for the purified recombinant *At*GABA-T

Parameters were determined from a single typical preparation, and represent the calculated mean ±SE for the best fit of data to the Michaelis–Menten equation by non-linear regression. The forward reaction utilizes GABA and pyruvate or glyoxylate to generate SSA and alanine or glycine. The reverse reaction uses alanine with SSA or glyoxylate to produce pyruvate and GABA or glycine.

Varied substrate	Fixed substrate	K_m (mM)	V_{max} (μmol mg^{-1} protein min^{-1})	k_{cat} (s^{-1})	k_{cat}/K_m (s^{-1} mM^{-1})
Forward					
GABA	Pyruvate	0.34±0.02	11.9±0.2	10.6	31
GABA	Glyoxylate	0.18±0.01	7.8±0.1	6.9	39
Pyruvate	GABA	0.14±0.01	11.9±0.2	10.6	76
Glyoxylate	GABA	0.11±0.01	10.9±0.3	9.7	88
Reverse					
Alanine	SSA	2.4±0.3	17.4±0.6	15.4	6.4
Alanine	Glyoxylate	2.2±0.3	15.8±0.6	14.1	6.5
SSA	Alanine	0.014±0.002	12.1±0.5	10.8	770
Glyoxylate	Alanine	0.14±0.02	13.6±0.4	12.1	86

Table 3. Inhibition constants for various inhibitors of pyruvate-dependent *At*GABA-T activity

Parameters were determined from a single typical preparation, and represent the calculated mean ±SE for the best fit of data to the appropriate Michaelis–Menten equation by non-linear regression.

Inhibitor	K_i (mM)
β-Alanine	0.55±0.13
Ornithine	0.46±0.12
Vigabatrin	0.62±0.16
Glycine	3.70±0.46

Subcellular localization of Arabidopsis *GABA-T*

In order to determine the subcellular localization of *At*GATA-T, GFP was fused to its C-terminus and the resulting fusion protein (*At*GABA-T–GFP) was expressed transiently in tobacco BY-2 suspension-cultured cells serving as a well-characterized *in vivo* import system (Banjoko and Trelease, 1995; Miao and Jiang, 2007). Figure 3A–C shows that *At*GABA-T–GFP expressed in BY-2 cells displayed a punctate fluorescence pattern that was identical to the fluorescence pattern attributable to co-expressed βATPase–CAT, a well-established mitochondrial matrix marker protein (Chaumont *et al.*, 1994). Similar co-localization was observed for expressed *At*GABA-T–GFP and immunostained endogenous E1β, a subunit of the pyruvate dehydrogenase complex located in the mitochondrial matrix (Luethy *et al.*, 2001) (Supplementary Fig. S5A–C at *JXB* online). A C-terminal myc epitope-tagged version of *At*GABA-T (*At*GABA-T-myc) also co-localized with co-expressed mitochondrial βATPase–CAT in BY-2 cells (Supplementary Fig. S5D–F at *JXB* online), indicating that the appended GFP moiety in *At*GABA-T–GFP did not influence *At*GABA-T localization. Figure 3 also shows that the putative N-terminal pre-sequence of *At*GABA-T, consisting of residues 1–36 plus 10 immediately adjacent residues, fused to GFP (1–46-*At*GABA-T–GFP), exhibited an identical localization to co-expressed mitochondrial βATPase–CAT (Fig. 3D–F). In contrast, when the N-terminal 46 residues were deleted from *At*GABA-T–GFP, the resulting truncated fusion protein (1–46Δ*At*GABA-T–GFP) accumulated throughout the cytosol and nucleus (Fig. 3G–I).

To confirm that *At*GABA-T was imported into mitochondria, BY-2 cells transiently expressing *At*GABA-T-myc were treated with Triton X-100 or digitonin to permeabilize cellular membranes selectively (Lee *et al.*, 1997). Incubation of cells with Triton X-100 perforates all cellular membranes, including the plasma membrane and organellar membranes, allowing for the immunodetection of both endogenous E1β in the mitochondrial matrix and α-tubulin in the cytosol (Fig. 4A–C). Incubation of cells with digitonin, however, perforates only the plasma membrane, allowing for the immunodection of cytosolic α-tubulin, but not organelle (mitochondrial) membrane-protected E1β (Fig. 4D–F). While transiently

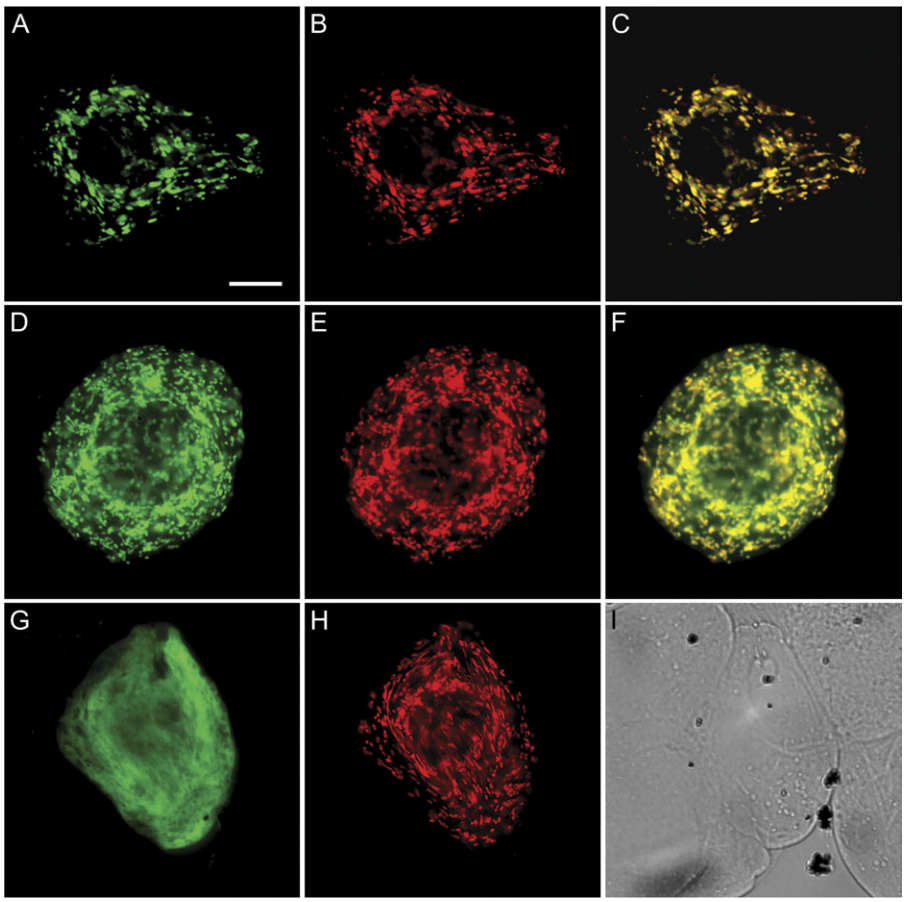

Fig. 3. Localization of *At*GABA-T–GFP to mitochondria in tobacco BY-2 cells is mediated by its N-terminal 46 amino acid pre-sequence. Co-transiently expressed *At*GABA-T–GFP (A) and the mitochondrial marker protein βATPase–CAT (B) co-localize in the same BY-2 cell, as evidenced by the yellow colour in the merged image (C). 1–46-*At*GABA-T–GFP (D) co-localizes with co-expressed βATPase–CAT (E) in mitochondria in the same BY-2 cell, as evidenced by the yellow colour in the merged image (F). Expressed 1–46Δ*At*GABA-T–GFP localizes throughout the cytosol and nucleus (G) and not to βATPase–CAT-containing mitochondria in the same co-transformed BY-2 cell (H). (I) Differential interference contrast (DIC) image of the same cell shown in (G) and (H). Bar in (A)=10 μm.

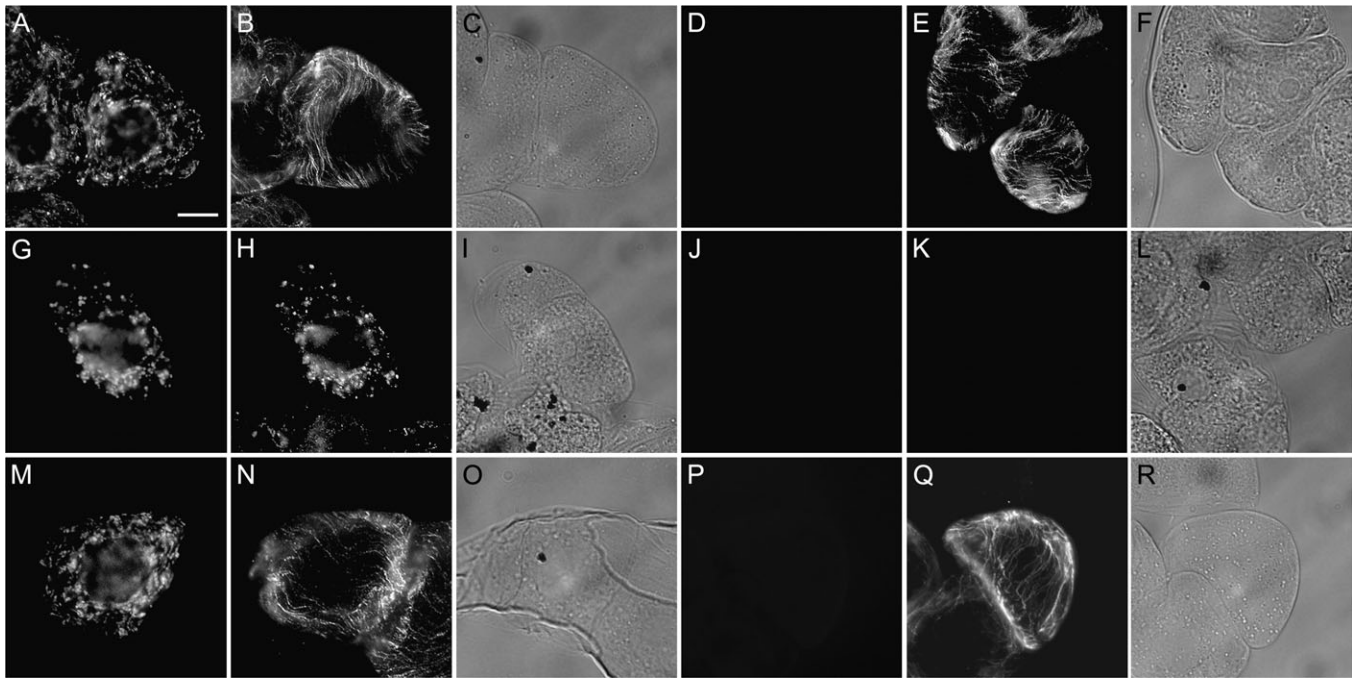

Fig. 4. Differential permeabilization of *At*GABA-T-myc-transformed tobacco BY-2 cells. The presence or absence of immunofluorescence in differential permeabilized cells indicates whether applied antibodies had access to transiently expressed *At*GABA-T-myc and endogenous E1β within mitochondria or endogenous α-tubulin in the cytosol. Non-transformed (A–F) or *At*GABA-T-myc transiently transformed (G–R) cells were fixed and permeabilized using either Triton X-100 (A–C, G–I, and M-O), which permeabilizes all cellular membranes, or digitonin (D–F, J–L, and P–R), which selectively permeabilizes the plasma membranes, then cells were processed for immunofluorescence microscopy. Immunostaining of endogenous E1β in the matrix of mitochondria (A) and of α-tubulin in cytosolic microtubules (B) in the same non-transformed, Triton X-100-permeabilized cells. Lack of immunostaining of endogenous E1β (D), but the presence of cytosolic tubulin (E), in the same digitonin-permeabilized cells. Immunostaining of expressed *At*GABA-T-myc (G and M) and endogenous E1β (H) and tubulin (N) in the same Triton X-100-permeabilized cells. Lack of immunostaining of expressed *At*GABA-T-myc (J and P) and endogenous E1β (K), but the presence of cytosolic tubulin (Q), in the same digitonin-permeabilized cells. Differential interference contrast (DIC) images of the corresponding BY-2 cells are shown in (C, F, I, L, O, and R). Bar in (A)=10 μm.

expressed *At*GABA-T-myc was immunodetected along with endogenous E1β in Triton X-100-permeabilized cells (Fig. 4G–I), neither protein was immunodetected in BY-2 cells permeabilized with digitonin (Fig. 4J–L). Likewise, both expressed *At*GABA-T-myc and endogenous tubulin were immunodetected in cells that were permeabilized with Triton X-100 (Fig. 4M–O), whereas only tubulin was immunodetected in digitonin-treated cells (Fig. 3P–R). Taken together, the data presented in Figs 3 and 4 indicate that *At*GABA-T is targeted to and imported into mitochondria in BY-2 cells via an N-terminal pre-sequence.

Characterization of native Arabidopsis *GABA-T*

To confirm the presence of glyoxylate-dependent activity *in planta*, crude cell-free extracts of *Arabidopsis* leaves from two ecotypes were assayed for GABA-T activity. Both pyruvate- and glyoxylate-dependent GABA-T activities were present in wild-type *Arabidopsis*, but not in the corresponding knockout mutants (Table 4). Growth of the knockout mutants on minimal medium containing GABA

Table 4. Native GABA-T activity in cell-free extracts of two *Arabidopsis* ecotypes (Columbia and Wassilewskija) and corresponding knockout mutants

Data represent the mean ±SE of three preparations. Weight was expressed on an area basis by considering 0.018 g of fresh mass to be equivalent to 1 cm^2. ND, indicates not detected; the lower limit of detection for the method was 0.25 nmol g^{-1} fresh mass min^{-1}.

Ecotype/ mutant	Amino acceptor	Specific activity (nmol g^{-1} fresh mass min^{-1})	Specific activity (nmol m^{-2} s^{-1})
Columbia			
Wild type	Pyruvate	13.98±0.37	41.99±1.10
GABAT1-1	Pyruvate	ND	ND
Wild type	Glyoxylate	8.13±0.51	24.42±1.53
GABAT1-1	Glyoxylate	ND	ND
Wassilewskija			
Wild-type	Pyruvate	17.07±0.85	51.27±2.55
POP2-3	Pyruvate	ND	ND
Wild-type	Glyoxylate	7.73±0.25	23.21±0.75
POP2-3	Glyoxylate	ND	ND

as the sole N source revealed a white, bleached phenotype despite the presumed presence of 2-oxoglutarate-dependent activity (Fig. 5). Indeed, under these conditions, the knockout mutant appeared to exhibit a much shorter life cycle than when grown on minimal medium with no N. The GABAT1-1 knockout mutant also possessed an elevated concentration of leaf GABA, together with smaller but still significant increases in glutamine and methionine (Fig. 6), providing further evidence for the inability of these plants to catabolize GABA. Previous work demonstrated that GABA levels in the POP2-3 mutant are 11-fold higher than those in the wild type (Palanivelu *et al.*, 2003).

The GABA-T transcript was present in all plant organs analysed, and its relative abundance in those organs was reasonably consistent between experiments (Fig. 7). For leaves, transcript abundance increased with development, although the level in senescent tissue was not as high as that in roots. Young leaves and stems, and mature leaves and flowers displayed similar levels.

Discussion

Previous research demonstrated production of the full-length *At*GABA-T in *E. coli* using the Xpress™ protein expression system (Invitrogen); however, the expression level in *E. coli* was low and could only be detected on gels using blotting techniques (Van Cauwenberghe *et al.*, 2002). In the present study, it was possible to increase expression of the full-length *At*GABA-T by using the pET15B expression vector (Novagen) with *E. coli* BL21 (DE3) Rosetta pLysS cells, but the protein formed insoluble aggregates. Efforts to improve the recovery of soluble *At*GABA-T (i.e. reducing the temperature during the induction period, lengthening the induction period, lowering the IPTG concentration, and supplementation of the medium with ethanol) were unsuccessful (data not shown). However, co-expression of the GroES/GroEL chaperone complex, as well as removal of the putative mitochondrial targeting pre-sequence, dramatically enhanced the recovery of recombinant *At*GABA-T in the soluble form (Fig. 1A, B; Table 1). Increased soluble expression using the chaperone complex is a well-documented phenomenon (Dale *et al.*, 1994; Tibbetts and Appling, 2000; Mitsuda and Iwasaki, 2006). Furthermore, the targeting pre-sequence is probably removed from the mature protein upon localization within the cell (Glaser *et al.*, 1998). Expression of a truncated *At*GABA-T lacking the targeting pre-sequence should therefore reflect the mature enzyme *in planta* and has the added benefit of providing increased levels of expression and solubility in *E. coli*.

Previous biochemical analysis demonstrated that the recombinant *At*GABA-T possesses pyruvate-, but not 2-oxoglutarate-dependent activity (Van Cauwenberghe *et al.*, 2002). In the present report, it was demonstrated that the enzyme catalysed irreversible glyoxylate-dependent, as well as reversible pyruvate-dependent GABA-T activity (Table 2, Supplementary Figs S2, S3 at *JXB* online). To our knowledge, this is the first report of glyoxylate-dependent GABA-T activity in any species. 2-Oxoglutarate-dependent GABA-T in mammals, fungi, and bacteria is widely documented (Buzenet *et al.*, 1978; Maitre *et al.*, 1978; Der Garabedian *et al.*, 1986; Kumar and Punekar, 1997; Liu *et al.*, 2004), and pyruvate-dependent GABA-T (β-alanine also serves as an amino donor) activity in bacteria and fungi has been reported (Yonaha *et al.*, 1983). Analysis of the amino acid composition in flowers of *Arabidopsis* GABA-T knockout mutants revealed a 5.7-fold enhancement in β-alanine concentration, together with a 100-fold increase in GABA (Palanivelu *et al.*, 2003). While this could be interpreted as

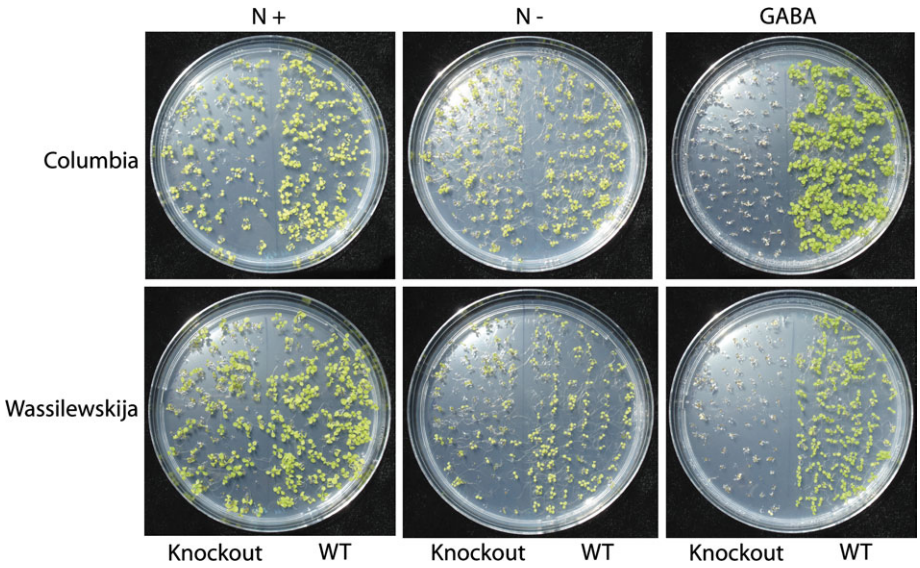

Fig. 5. Growth of wild-type seedlings and knockout mutants (GABA-T1-1 and POP2-3) of *Arabidopsis* (ecotypes Columbia and Wassilewskija, respectively) on minimal MS medium containing GABA as the sole source of N (right panels), minimal MS medium with no source of N (centre panels B), and standard MS medium with N (left panels). Similar results were obtained in a replicated experiment.

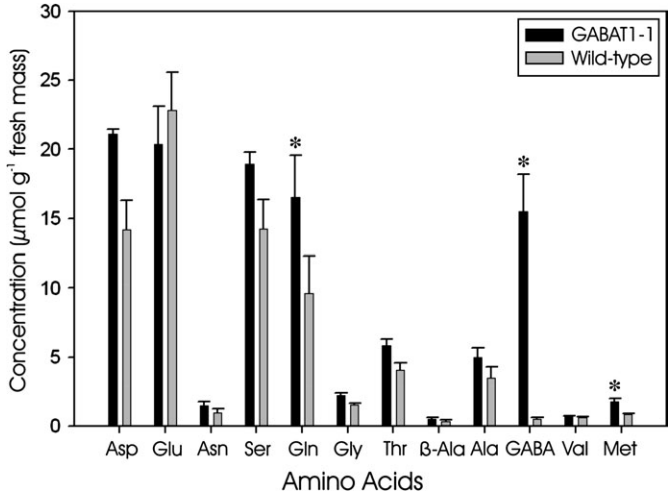

Fig. 6. Amino acid profile of mature leaves from *Arabidopsis* Columbia wild type and the GABA-T knockout (GABA-T1-1). Data represent the mean ±SE of three plants. Significant differences between the wild type and mutants, based on the Student's *t*-test ($P \leqslant 0.05$), are indicated with an asterisk.

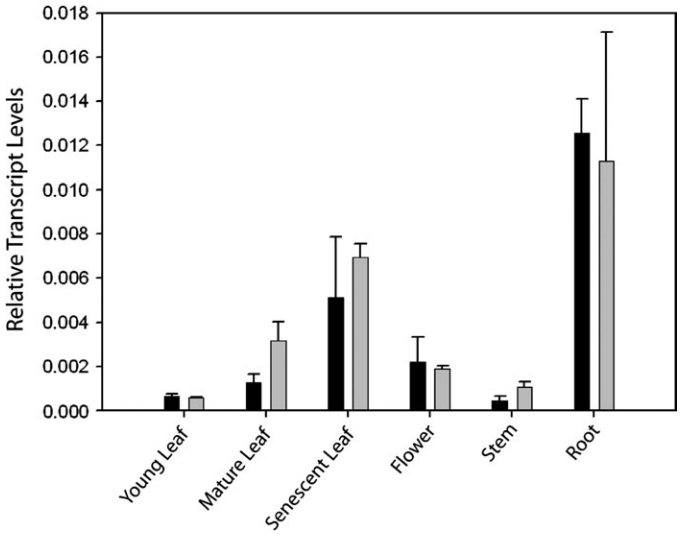

Fig. 7. Relative GABA-T transcript abundance in various organs of wild-type *Arabidopsis* plants. The results are from two separate experiments (open and filled bars). Data represent the mean ±SE of three plants.

evidence for a promiscuous transaminase that utilizes both GABA and β-alanine, the evidence presented here indicates that the recombinant *At*GABA-T does not utilize β-alanine. Indeed, the enzyme utilizes GABA and alanine only as amino donors for the forward and reverse reactions, respectively (Table 2).

The dual specificity of *At*GABA-T could be considered analagous to that found with *Arabidopsis* alanine:glyoxylate (AGT1) and glutamine:glyoxylate (GGT1 and GGT2) aminotransferase. AGT1 exhibits three activities: serine:glyoxylate, serine:pyruvate, and alanine:glyoxylate, with the K_m value for alanine (101 mM) being rather high, making its physiological relevance questionable (Liepman and Olsen, 2001). The homologues GGT1 and GGT2 also exhibit substrate promiscuity, catalysing glutamate:glyoxylate, alanine:glyoxylate, glutamate:pyruvate, and alanine:2-oxoglutarate activities (Liepman and Olsen, 2003). Thus, there is a tendency for plant glyoxylate-dependent transaminases to utilize multiple substrates.

The kinetic parameters for pyruvate and glyoxylate were similar (Table 2), indicating that the enzyme could utilize either substrate interchangeably. SSA, the amino acceptor for the reverse reaction, was the most efficient substrate for the enzyme, exhibiting a specificity constant that was an order of magnitude lower than for both pyruvate and glyoxylate. The calculated equilibrium ratio of 0.68 for the pyruvate-dependent reaction indicates that the reverse reaction is slightly favoured. This observation is similar to previous reports for GABA-Ts from rat, *Pseudomonas*, and mouse, which all favour the reverse direction to varying degrees (see Van Bemmelen *et al.*, 1985). While the reverse reaction is favoured *in vitro*, two lines of evidence suggest that the enzyme does not generate much, if any, GABA *in planta*: (i) GABA synthesis and accumulation is highly regulated via stress stimulation/activation of glutamate decarboxylase (Crawford *et al.*, 1994; Snedden *et al.*, 1995, 1996); and (ii) the loss or inhibition of GABA-T activity causes the accumulation of GABA (Fig. 6; Palanivelu *et al.*, 2003; Fait *et al.*, 2005). The affinity of the enzyme for SSA could serve as a safety mechanism to ensure that SSA does not accumulate in the mitochondrion (Lindahl, 1992), a hypothesis that is consistent with the regulation of *Arabidopsis* SSADH by adenine nucleotides (Busch and Fromm, 1999). The irreversibility of the glyoxylate-dependent reaction is not likely to be due to specific exclusion of glycine by the enzyme, but rather a general transaminase phenomenom related to a high energy requirement for the reverse reaction (Smith, 1985). Indeed, glycine acted as a competitive inhibitor for the reaction, with a K_i value similar to the K_m for alanine, indicating that the molecule fits into the active site (Table 3).

Vigabatrin was an effective competitive inhibitor of GABA-T activity (Table 3, Supplementary Fig. S4 at *JXB* online) as one would expect given its effectiveness as an inhibitor in mammalian systems (De Biase *et al.*, 1991) and its ability to reduce the accumulation of reactive oxygen intermediates in SSADH-deficient *Arabidopsis* plants (Fait *et al.*, 2005). Both β-alanine and ornithine also competitively inhibited GABA-T activity (Table 3), with K_i values similar to that for vigabatrin, strongly suggesting that all three compounds inhibit the enzyme because of their structural similarity to GABA.

A mitochondrial localization for GABA-T was previously indicated by cell fractionation studies (Breitkruez and Shelp, 1995) and mitochondrial proteome analysis (Sweetlove *et al.*, 2002). This localization was confirmed in the present study by the transient expression of the full-length *AtGABA-T* cDNA in tobacco BY-2 cells. Herein, *At*GABA-T co-localized with the co-expressed mitochondrial marker proteins βATPase–CAT (Chaumont *et al.*, 1994) or E1β (Luethy *et al.*, 2001), regardless of whether it was appended to the

GFP or myc epitope tag (Fig. 3; Supplementary Fig. S5 at *JXB* online). Differential permeabilization of cellular membranes using Triton-X100 and digitonin also confirmed that *At*GABA-T was localized inside the mitochondrion rather than associated with the outer membrane (Fig. 4). In addition, when the predicted *At*GABA-T N-terminal pre-sequence (i.e. 36 amino acid residues plus 10 immediately adjacent amino acids) was appended to GFP, the fusion protein (1–46-*At*GABA-T–GFP) sorted to mitochondria, whereas the corresponding truncated version of *At*GABA-T (1–46Δ*At*GABA-T–GFP), which lacks the N-terminal targeting pre-sequence, was localized to the cytosol and nucleoplasm (Fig. 3). These latter observations are consistent with previous reports of untargeted GFP in the nucleus and cytosol of plant cells (Köhler *et al.*, 1997), and that the loss of *At*GABA-T's mitochondria targeting ability was due to the removal of its N-terminal pre-sequence.

The absence of both pyruvate- and glyoxylate-dependent GABA-T activities in knockout mutants, and the inability of these mutants to grow on GABA as the sole N source, established that the protein under consideration catalyses GABA-T activity *in planta* (Table 4; Fig. 5). This indicates that *Arabidopsis* contains only one pyruvate-dependent GABA-T and does not contain a cytosolic form as predicted for rice (Ansari *et al.*, 2005), tomato (AY240230), and pepper (AAC78480). These results, in conjunction with the accumulation of GABA in the knockouts (Fig. 6; Palanivelu *et al.* 2003), also suggest that a separate 2-oxoglutarate-dependent GABA-T is not present in seedlings, even though cell-free *Arabidopsis* leaf extracts displayed a low level of 2-oxoglutarate-dependent activity (Table 1), similar to that previously found in tobacco (Van Cauwenberghe and Shelp, 1999). The most likely explanation is that plants lack a second GABA-T enzyme and that the detectable 2-oxoglutarate-dependent activity is actually a combination of pyruvate-dependent GABA-T and alanine:2-oxoglutarate aminotransferase activity (Barbosa, 2002). This hypothesis is consistent with the instability of, and difficulty in purifying, the 2-oxoglutarate-dependent GABA-T from tobacco, which could not actually be separated from the more abundant pyruvate-dependent activity (Van Cauwenberghe and Shelp, 1999), the failure to identify a 2-oxoglutarate-dependent GABA-T in *Arabidopsis* based on homology (Barbosa, 2002), and the prevention of SSA and γ-hydroxybutyrate accumulation in the *ssadh* knockout by complementation with pyruvate-dependent GABA-T knockouts (Ludewig *et al.*, 2008). In most cases, 2-oxoglutarate-dependent GABA-T activity in crude cell-free extracts is reported as lower than pyruvate-dependent activity; indeed, it is often over an order of magnitude lower (Table 1; also see references in Van Cauwenburghe and Shelp, 1999). These results may be due to the operation of pyruvate-dependent GABA-T in insufficiently desalted extracts, thereby allowing the coupled reaction to occur. The one exception is a recent paper by Akihiro *et al.* (2008), which reported that 2-oxoglutarate-dependent GABA-T activity in tomato fruit is three orders of magnitude higher than pyruvate-dependent activity. There are two reasons to treat those results with caution: (i) the pyruvate-dependent activity was assayed with 10 mM pyruvate, which is well above levels known to inhibit the enzyme (Van Cauwenberghe and Shelp, 1999); and (ii) the two activities were assayed under different conditions, with 2-oxogluarate-dependent activity being monitored after a 12 h incubation.

*At*GABA-T knockout mutants of *Arabidopsis* grown with GABA as the sole N source developed a white bleached phenotype that was not observed in seedlings grown without N (Fig. 5). This might be attributed to the promotion of plant growth by GABA, followed by premature death due to the plant's inability to catabolize GABA. While further experimentation is required to test this hypothesis, it does fit with the recent literature suggesting a role for GABA in signalling (see Bouché *et al.*, 2003; Shelp *et al.*, 2006). GABA receptors have not yet been identified in plants; however, the presence of GABA-binding sites on pollen and somatic protoplast membranes has been demonstrated (Yu *et al.*, 2006).

*At*GABA-T knockout mutants of *Arabidopsis* display only one obvious physical phenotype, reduced seed production under self-fertilization, implying that the role of this enzyme is restricted to flower tissue (Palanivelu *et al.*, 2003). More recently, it has been demonstrated that *At*GABA-T knockouts also fail to respond to treatment with the C6-volatile E-2-hexanol (Mirabella *et al.*, 2008), although the role of GABA in C6-volatile signalling is unknown. Real-time PCR analysis of the *At*GABA-T transcript in *Arabidopsis* revealed that the gene was expressed in all organs tested, including roots, stem, leaves, and flowers (Fig. 7). In leaves, there was a clear trend of increasing expression with development, a pattern similar to that found in rice (Ansari *et al.*, 2005). Roots contained the highest level of *At*GABA-T transcript, though the physiological purpose for that level is not yet known. These results are in agreement with a previous study of *At*GABA-T expression in all tissues except those for roots, which were found to have the same level as stem and mature leaf tissue (Miyashita and Good, 2008). Differences in *At*GABA-T expression in roots between the two studies might be attributed to the growth conditions (semi-hydroponics versus soil). Nevertheless, the expression of *At*GABA-T throughout the *Arabidopsis* plant indicates that it has a function(s) beyond pollen tube guidance in flowers (Palanivelu *et al.*, 2003).

Identification of glyoxylate-dependent GABA-T activity raises the question of its role in plants. The mitochondrion is not traditionally associated with glyoxylate transamination. However, a glycolate dehydrogenase exists in *Arabidopsis* mitochondria, which resembles the photorespiratory pathway employed in green algae (Bari *et al.*, 2004; Stabenau and Winkler, 2005). This enzyme could provide a source of glyoxylate for GABA-T, providing the basis for a link between GABA metabolism and photorespiration. Theoretically, these two enzymes could allow the glycolate to glycine reactions of photorespiration to occur in mitochondria. It is noteworthy that knockouts of both glycolate dehydrogenase (Bari *et al.*, 2004) and GABA-T (this study)

fail to exhibit typical photorespiration phenotypes when grown under atmospheric conditions. Despite the lack of phenotype, Niessen *et al.* (2007) demonstrated that glycolate dehydrogenase knockouts have a reduced photorespiration capacity. Sharkey (1988) estimated, based on Rubisco kinetics, that the rate of photorespiration at 210 μmol mol^{-1} CO_2 is 8 μmol m^{-2} s^{-1}, which compares with a GABA-T activity with 1 mM substrate and optimum pH of 40–50 nmol m^{-2} s^{-1} (equivalent to 17–20 μmol mg^{-1} protein min^{-1}) in *Arabidopsis* crude cell-free extracts (Table 4). Thus, the GABA-T activity is at least two orders of magnitude lower than the expected rate of photorespiration, indicating that the theoretical contribution of GABA-T to photorespiratory flux would be small. Unfortunately, the glycolate dehydrogenase activity extracted from *Arabidopsis* is reported on a crude protein basis only (310 mmol mg^{-1} protein min^{-1}; Niessen *et al.*, 2007), which is extremely high compared with reports of algal glycolate dehydrogenase, which are in the nmol mg^{-1} min^{-1} range (Stabenau and Winkler, 2005).

Photorespiration has been proposed to act as a mechanism for stress protection in plants, preventing the over-reduction of the photosynthetic electron chain and photoinhibition, and providing metabolites such as glycine for other processes such as the synthesis of glutathione (Kozaki and Takebo, 1996; Wingler *et al.*, 2000; Mullineaux and Rausch, 2005, and references therein). A mitochondrial version of the photorespiratory pathway would bypass the H_2O_2 production associated with the glycolate oxidase reaction, and reduce generation of additional reactive oxygen species. The accumulation of GABA during stress is a well documented phenomenom (Bown and Shelp, 1989; Satya Narayan and Nair, 1990; Bown and Shelp, 1997; Shelp *et al.*, 1999; Kinnersley and Turano, 2000) and would provide ample amino donor for the transamination of glyoxylate to glycine during stress. While a model in which GABA metabolism contributes to photorespiration is very appealing, the lack of a photorespiration phenotype for both glycolate dehydrogenase and *At*GABA-T knockout mutants suggests caution. Any contribution of *At*GABA-T to photorespiration is likely to occur under stress when CO_2 availability is restricted. Perhaps *At*GABA-T functions to prevent the cellular accumulation of glyoxylate, a metabolite that is highly reactive and known to inhibit Rubisco activity (Campbell and Ogren, 1990; Hausler *et al.*, 1996). Future work utilizing ^{15}N-labelled GABA to determine the fate of GABA-N *in planta* under conditions designed to manipulate photorespiration may provide a better understanding of the relationship between the two pathways.

Supplementary data

Supplementary data can be found at *JXB* online.

Table S1. Synthetic oligonucleotide primers used to amplify GABA-T sequences containing *Nhe*I restrictions sites.

Materials and methods. Production and purification of recombinant *E. coli* succinic semialdehyde dehydrogenase.

Figure S1. SDS-PAGE analysis of expression and purification of the recombinant *E. coli* K-12 SSADH from BL21 (DE3) Rosetta pLysS cells co-expressing the GroES/EL chaperone complex.

Figure S2. Kinetic characterization of *At*GABA-T activity in the forward direction.

Figure S3. Kinetic characterization of *At*GABA-T activity in the reverse direction.

Figure S4. Inhibition of pyruvate-dependent *At*GABA-T activity by (A) β-Ala, (B) Orn, (C) vigabatrin, and (D) Gly.

Figure S5. Localization of *At*GABA-T–GFP and *At*GABA-T-myc to mitochondria in tobacco BY-2 cells.

Acknowledgements

This research was supported by Discovery Grants from the Natural Sciences and Engineering Research Council of Canada (NSERC) to RTM and BJS, and the Ontario Ministry of Agriculture and Food to BJS, and postgraduate awards from the Ontario Graduate Scholarships Program to SMC, RD, and PKD. The authors thank F Chaumont (University of Louvain) for pBIN35Sb60catE9, Jan Miernyk (University of Missouri-Columbia) for rabbit pea-E1β antibodies, and Andrew Hanson (University of Florida) for suggesting use of the GroES/EL chaperone. The authors would also thank the Arabidopsis Biological Resource Center for providing us with POP2-3 seeds, and Yo Miyashita (University of Alberta) for providing GABAT1-1 seeds, which were originally obtained from the Arabidopsis Biological Resource Center.

References

Akihiro T, Koike S, Tani R, *et al*. 2008. Biochemical mechanism on GABA accumulation during fruit development in tomato. *Plant and Cell Physiology* **49,** 1378–1389.

Allan WL, Peiris C, Bown AW, Shelp BJ. 2003. Gamma-hyroxybutyrate accumulates in green tea and soybean sprouts in response to oxygen deficiency. *Canadian Journal of Plant Science* **83,** 951–953.

Allan WL, Shelp BJ. 2006. Fluctuations of γ-aminobutyrate, γ-hydroxybutyrate and related amino acids in *Arabidopsis* leaves as a function of the light–dark cycle, leaf age and N stress. *Canadian Journal of Botany* **84,** 1339–1346.

Allan WL, Simpson JP, Clark SM, Shelp BJ. 2008. γ-Hydroxybutyrate accumulation in *Arabidopsis* and tobacco plants is a general response to abiotic stress: putative regulation by redox balance and glyoxylate reductase isoforms. *Journal of Experimental Botany* **59,** 2555–2564.

André B, Jauniaux J-C. 1990. Nucleotide sequence of the yeast *UGA1* gene encoding GABA transaminase. *Nucleic Acids Research* **18,** 3046.

Ansari IM, Lee R, Chen SG. 2005. A novel senescence-associated gene encoding γ-aminobutyric acid (GABA):pyruvate transaminase is unregulated during rice leaf senescence. *Physiologia Plantarum* **123,** 1–8.

Banjoko A, Trelease RN. 1995. Development and application of an *in vivo* plant peroxisome import system. *Plant Physiology* **107,** 1201–1208.

Barbosa JMF. 2002. Physiological, biochemical and molecular aspects of γ-aminobutyric acid (GABA): a stress-responsive non-protein amino acid. PhD thesis. Auburn: Auburn University.

Bari R, Kebeish R, Kalamajka R, Rademacher T, Peterhansel C. 2004. A glycolate dehydrogenase in the mitochondria of *Arabidopsis thaliana*. *Journal of Experimental Botany* **55,** 623–630.

Bartsch K, von Johnn-Marteville A, Schulz A. 1990. Molecular analysis of two genes of the *Escherichia coli gab* cluster: nucleotide sequence of the glutamate:succinic semialdehyde transaminase (*gabT*) and characterization of the succinic semialdehyde dehydrogenase (*gabD*). *Journal of Bacteriology* **172,** 7035–7042.

Baum G, Chen Y, Arazi T, Takatsuji H, Fromm H. 1993. A plant glutamate decarboxylase containing a calmodulin binding domain. *Journal of Biological Chemistry* **268,** 19610–19617.

Bouché N, Lacombe B, Fromm H. 2003. GABA signaling: a conserved and ubiquitous mechanism. *Trends in Cell Biology* **13,** 607–610.

Bouché N, Fromm H. 2004. GABA in plants: just a metabolite? *Trends in Plant Science* **9,** 110–115.

Bown AW, Shelp BJ. 1989. The metabolism and physiological roles of 4-aminobutyric acid. *Biochemistry (Life Science Advances)* **8,** 21–25.

Bown AW, Shelp BJ. 1997. The metabolism and functions of γ-aminobutyric acid. *Plant Physiology* **115,** 1–5.

Bradford M. 1976. A rapid and sensitive method for the quantitation of microgram quantities of protein utilizing the principle of protein–dye binding. *Analytical Biochemistry* **72,** 248–254.

Breitkreuz KE, Allan WA, Van Cauwenberghe OR, Jakobs C, Talibi D, André B, Shelp BJ. 2003. A novel γ-hyrdoxybutyrate dehydrogenase. Identification and expression of an Arabidopsis cDNA and potential role under oxygen deficiency. *Journal of Biological Chemistry* **278,** 41552–41556.

Breitkreuz KE, Shelp BJ. 1995. Subcellular compartmentation of the 4-aminobutyrate shunt in protoplasts from developing soybean cotyledons. *Plant Physiology* **108,** 99–103.

Busch KB, Fromm H. 1999. Plant succinic semialdehyde dehydrogenase. Cloning, purification, localization in mitochondria, and regulation by adenine nucleotides. *Plant Physiology* **121,** 589–597.

Buzenet AM, Fages C, Bloch-Tardy M, Gonnard P. 1978. Purification and properties of 4-aminobutyrate 2-ketoglutarate aminotransferase from pig liver. *Biochimica et Biophysica Acta* **522,** 400–411.

Campbell WJ, Ogren WL. 1990. Glyoxylate inhibition of ribulosebisphosphate carboxylase/oxygenase activation in intact, lysed, and reconstituted chloroplasts. *Photosynthesis Research* **23,** 257–268.

Chaumont F, de Castro Silva Filho M, Thomas D, Leterme S, Boutry M. 1994. Truncated presequences of mitochondrial F_1-ATPase β subunit from *Nicotiana plumbaginifolia* CAT and GUS proteins into mitochondria of transgenic tobacco. *Plant Molecular Biology* **24,** 631–641.

Chiu W, Niwa Y, Zeng W, Hirano T, Kobayashi H, Sheen J. 1996. Engineered GFP as a vital reporter in plants. *Current Biology* **6,** 325–330.

Crawford LA, Bown AW, Breitkreuz KE, Guinel FC. 1994. The synthesis of γ-aminobutyric acid in response to treatments reducing cytosolic pH. *Plant Physiology* **104,** 865–871.

Dale GE, Schonfield H-J, Langen H, Stieger M. 1994. Increased solubility of trimethoprim-resistant type S1 DHFR from *Staphylococcus aureus* in *Escherichia coli* cells overproducing the chaperonins GroEL and GroES. *Protein Engineering* **7,** 925–931.

De Biase D, Barre D, Bossa F, Pucci P, John RA. 1991. Chemistry of the inactivation of 4-aminobutyrate aminotransferase by the antiepileptic drug vigabatrin. *Journal of Biological Chemistry* **266,** 20056–20061.

De Biase D, Barra D, Simmaco M, John RA, Bossa F. 1995. Primary structure and tissue distribution of human 4-aminobutyrate aminotransferase. *European Journal of Biochemistry* **227,** 476–480.

Der Garabedian PA, Lotti AM, Vermeersch J. 1986. 4-Aminobutyrate:2-oxoglutarate aminotransferase from Candida: purification and properties. *European Journal of Biochemistry* **156,** 589–596.

Fait A, Fromm H, Walter D, Galili G, Fernie AR. 2008. Highway or byway: the metabolic role of the GABA shunt in plants. *Trends in Plant Science* **13,** 14–19.

Fait A, Yellin A, Fromm H. 2005. GABA shunt deficiencies and accumulation of reactive oxygen intermediates: insight from Arabidopsis mutants. *FEBS Letters* **579,** 415–420.

Fritze CE, Anderson TR. 2000. Epitope tagging: general method for tracking recombinant proteins. *Methods in Enzymology* **327,** 3–16.

Glaser E, Sjöling S, Tanudji M, Whelan J. 1998. Mitochondrial protein import in plants. Signals, sorting, targeting and regulation. *Plant Molecular Biology* **38,** 311–338.

Hausler RE, Bailey KJ, Lea PJ, Leegood RC. 1996. Control of photosynthesis in barley mutants with reduced activities of glutamine synthetase and glutamate synthase. III. Aspects of glyoxylate metabolism and effects of glyoxylate on the activation state of ribulose-1,5-bisphosphate carboxylase-oxygenase. *Planta* **200,** 388–396.

Hoover GJ, Van Cauwenberghe OR, Breitkreuz KE, Clark SM, Merrill AR, Shelp BJ. 2007. Characteristics of an *Arabidopsis* glyoxylate reductase: general biochemical properties and substrate specificity for the recombinant protein, and developmental expression and implications for glyoxylate and succinic semialdehyde metabolism in planta. *Canadian Journal of Botany* **85,** 883–895.

Kinnersley AM, Turano FJ. 2000. Gamma aminobutyric acid (GABA) and plant responses to stress. *Critical Reviews of Plant Science* **19,** 479–509.

Köhler RH, Zipfel WR, Webb WW, Hanson MR. 1997. The green fluorescent protein as a marker to visualize plant mitochondria *in vivo*. *The Plant Journal* **11,** 613–621.

Kozaki A, Takebo G. 1996. Photorespiration protects C3 plants from photooxidation. *Nature* **384,** 557–560.

Kumar S, Punekar NS. 1997. The metabolism of 4-aminobutyrate (GABA) in fungi. *Mycological Research* **4,** 403–409.

Lee MS, Mullen RT, Trelease RN. 1997. Oilseed isocitrate lyases lacking their essential type 1 peroxisomal targeting signal are piggybacked to glyoxysomes. *The Plant Cell* **9,** 185–197.

Liepman AH, Olsen LJ. 2001. Peroxisomal alanine:glyoxylate aminotransferase (AGT1) is a photorespiratory enzyme with multiple substrates in *Arabidopsis thaliana*. *The Plant Journal* **25,** 487–498.

Liepman AH, Olsen LJ. 2003. Alanine aminotransferase homologs catalyze the glutamate:glyoxylate aminotransferase reaction in peroxisomes of *Arabidopsis*. *Plant Physiology* **131,** 215–237.

Lindahl R. 1992. Aldehyde dehydrogenases and their roles in carcinogenesis. *Critical Reviews in Biochemistry and Molecular Biology* **27,** 283–335.

Ling V, Snedden WA, Shelp BJ, Assman SM. 1994. Analysis of a soluble calmodulin binding protein from fava bean roots: identification of glutamate decarboxylase as a calmodulin activated enzyme. *The Plant Cell* **6,** 1135–1143.

Liu W, Peterson PE, Carter RJ, Zhou X, Langston JA, Fisher AJ, Toney MD. 2004. Crystal structure of unbound and aminooxyacetate-bound *Escherichia coli* γ-aminobutyrate aminotransferase. *Biochemistry* **34,** 10896–10905.

Ludewig F, Hüser A, Fromm H, Beauclair L, Bouché N. 2008. Mutants of GABA transaminase (POP2) suppress the severe phenotype of succinic semialdehyde dehydrogenase (*ssadh*) mutants in *Arabidopsis*. *PLoS ONE* **3**, e3383. doi:10.1371/journal.pone.0003383.

Luethy MH, David NR, Elthon TE, Miernyk JA, Randall DD. 1995. Characterization of a monoclonal antibody directed against the E1α subunit of plant mitochondrial pyruvate dehydrogenase. *Journal of Plant Physiology* **145,** 443–449.

Luethy MH, Gemel J, Johnston ML, Mooney BP, Miernyk JA, Randall DD. 2001. Developmental expression of the mitochondrial pyruvate dehydrogenase complex in pea (*Pisum sativum*) seedlings. *Physiologia Plantarum* **112,** 559–566.

Maitre M, Ciesielski L, Cash C, Mandel P. 1978. Comparison of the structural characteristics of the 4-aminobutyrate:2-oxoglutarate transaminase from rat and humna brain, and of their affinites for certain inhibitors. *Biochimica et Biophysica Acta* **522,** 385–399.

Miao YS, Jiang L. 2007. Transient expression of fluorescent fusion proteins in protoplasts of suspension cultured cells. *Nature Protocols* **2,** 2348–2353.

Mirabella R, Rauwerda H, Struys EA, Jakobs C, Triantaphylides C, Haring MA, Schurrink RC. 2008. The *Arabidopsis her1* mutant implicates GABA in E-2hexenal responsivness. *The Plant Journal* **52,** 197–213.

Mitsuda M, Iwasaki M. 2006. Improvement in the expression of CYP2B6 by co-expression with molecular chaperones GroES/EL in *Escherichia coli*. *Protein Expression and Purification* **46,** 401–405.

Miyashita Y, Good AG. 2008. Contribution of the GABA shunt in hypoxia-induced alanine accumulation in roots of *Arabidopsis thaliana*. *Plant and Cell Physiology* **49,** 92–102.

Mullineaux PM, Rausch T. 2005. Glutathione, photosynthesis and the redox regulation of stress-responsive gene expression. *Photosynthesis Research* **86,** 459–474.

Murphy MA, Phillipson BA, Baker A, Mullen RT. 2003. Characterization of the targeting signal of the Arabidopsis 22-kD integral peroxisomal membrane protein. *Plant Physiology* **133,** 813–828.

Nakai K, Kanehisa M. 1992. A knowledge base for predicting protein localization sites in eukaryotic cells. *Genomics* **14,** 897–911.

Nicot N, Hausman JF, Hoffmann L, Ie Evers D. 2005. Housekeeping gene selection for real-time RT-PCR normalization in potato during biotic and abiotic stress. *Journal of Experimental Botany* **56,** 2907–2914.

Niessen M, Thiruveedhi K, Rosenkranz R, Kebeish R, Hirsch HJ, Kreuzaler F, Peterhansel C. 2007. Mitochondrial glycolate oxidation contributes to photorespiration in higher plants. *Journal of Experimental Botany* **58,** 2709–2715.

Palanivelu R, Brass L, Edlund AF, Preuss D. 2003. Pollen tube growth and guidance is regulated by *POP2*, an Arabidopsis gene that controls GABA levels. *Cell* **114,** 47–59.

Sambrook J, Fritsch EF, Maniatis T. 1989. *Molecular cloning: a laboratory manual*, 2nd edn. Cold Spring Harbor, NY: Cold Spring Harbor Laboratory Press.

Satya Narayan V, Nair PM. 1990. Metabolism, enzymology and possible roles of 4-aminobutyrate in higher plants. *Phytochemistry* **29,** 367–375.

Sharkey TD. 1988. Estimating the rate of photorespiration in leaves. *Physiologia Plantarum* **73,** 147–152.

Shelp BJ, Bown AW, Faure D. 2006. Extracellular gamma-aminobutyrate mediates communication between plants and other organisms. *Plant Physiology* **142,** 1350–1352.

Shelp BJ, Bown AW, McLean MD. 1999. Metabolism and functions of gamma-aminobutyric acid. *Trends in Plant Science* **4,** 446–452.

Shelp BJ, Penner R, Zhu Z. 1992. Broccoli (*Brassica oleracea* var. *italica*) cultivar response to boron deficiency. *Canadian Journal of Plant Science* **72,** 883–888.

Shelp BJ, Walton CS, Snedden WA, Tuin LG, Oresnik IJ, Layzell DB. 1995. GABA shunt in developing soybean seeds is associated with hypoxia. *Physiologia Plantarum* **94,** 219–228.

Simpson JP, Di Leo R, Dhanoa PK, Allan WL, Makhmoudova A, Clark SM, Hoover GJ, Mullen RT, Shelp BJ. 2008. Identification and characterization of a plastid-localized Arabidopsis glyoxylate reductase isoform: comparison with a cytosolic isoform and implications for cellular redox homeostasis and aldehyde detoxification. *Journal of Experimental Botany* **59,** 2545–2554.

Sjöling S, Glaser E. 1998. Mitochondrial targeting peptides in plants. *Trends in Plant Science* **3,** 136–140.

Smith IK. 1985. Aminotransferases utilizing glyoxylate. In: Christen P, Metzler DE, eds. *Transaminases*. New York: Wiley, 390–396.

Snedden WA, Arazi T, Fromm H, Shelp BJ. 1995. Calcium/calmodulin activation of soybean glutamate decarboxylase. *Plant Physiology* **108,** 543–549.

Snedden WA, Koutsia N, Baum G, Fromm H. 1996. Activation of petunia glutamate decarboxylase by calcium/calmodulin or a monoclonal antibody which recognizes the calmodulin binding domain. *Journal of Biological Chemistry* **271,** 4148–4153.

Stabenau H, Winkler U. 2005. Glycolate metabolism in green algae. *Physiologia Plantarum* **123,** 235–245.

Sweetlove LJ, Heazlewood JL, Herald V, Holtzapffel R, Day DA, Leaver CJ, Millar AH. 2003. The impact of oxidative stress on *Arabidopsis* mitochondria. *The Plant Journal* **32,** 891–904.

Tibbetts AS, Applings DR. 2000. Characterization of two 5-amino-imidazole-4-carboxaminde ribonucleotide transformylase/inosine monophosphate cyclohydrolase isozymes from *Saccharomyces cerevisiae*. *Journal of Biological Chemistry* **275,** 20920–20927.

Trelease RN, Xie W, Lee MS, Mullen RT. 1996. Rat liver catalase is sorted to peroxisomes by its C-terminal tripeptide Ala-Asn-Leu, not by the internal Ser-Lys-Leu motif. *European Journal of Cell Biology* **71,** 248–258.

Van Bemmelen FJ, Schouten MJ, Fekkes D, Bruinvels J. 1985. Succinic semialdehyde as a substrate for the formation of γ-amino-butyric acid. *Journal of Neurochemistry* **45,** 1471–1474.

Van Cauwenberghe OR, Makhmoudova A, McLean MD, Clark S, Shelp BJ. 2002. Plant pyruvate-dependent gamma-aminobutyrate transaminase: identification of an *Arabidopsis* cDNA and its expression in *Escherichia coli*. *Canadian Journal of Botany* **80,** 933–941.

Van Cauwenberghe OR, Shelp BJ. 1999. Biochemical characterization of partially purified GABA:pyruvate transaminase from *Nicotiana tabacum*. *Phytochemistry* **52,** 575–581.

Wingler A, Lea PJ, Quick WP, Leegood RC. 2000. Photorespiration: metabolic pathways and their role in stress protection. *Philosophical Transactions of the Royal Society B: Biological Sciences* **355,** 1517–1529.

Yonaha K, Suziki K, Minei H, Toyama S. 1983. Distribution of ω-amino-acid:pyruvate transaminase and aminobutyrate:α-ketoglutarate transaminase in microorganisms. *Agricultural and Biological Chemistry* **47,** 2257–2265.

Yu G, Liang J, He Z, Sun M. 2006. Quantum dot-mediated detection of γ-aminobutyric acid binding sites on the surface of living protoplasts in tobacco. *Chemistry and Biology* **13,** 723–731.